Plant, Cell and Environment (2005) **28**, 389–401

Adjustment of leaf photosynthesis to shade in a natural canopy: reallocation of nitrogen

H. EICHELMANN[1], V. OJA[1], B. RASULOV[1], E. PADU[1], I. BICHELE[1], H. PETTAI[1], P. MÄND[2], O. KULL[2] & A. LAISK[1]

[1]*Department of Plant Physiology, Institute of Molecular and Cell Biology, University of, Tartu, Riia st. 23, Tartu 51010 Estonia and* [2]*Department of Applied Ecology, Institute of Botany and Ecology, University of Tartu, Lai st. 40, Tartu 51005 Estonia*

ABSTRACT

The present study was performed to investigate the adjustment of the constituents of the light and dark reactions of photosynthesis to the natural growth irradiance in the leaves of an overstorey species, *Betula pendula* Roth, a subcanopy species *Tilia cordata* P. Mill., and a herb *Solidago virgaurea* L. growing in a natural plant community in Järvselja, Estonia. Shoots were collected from the site and properties of individual leaves were measured in a laboratory, by applying a routine of kinetic gas exchange and optical measurements that revealed photosystem II (PSII), photosystem I (PSI), and cytochrome b_6f densities per leaf area and the distribution of excitation (or chlorophyll, Chl) between the two photosystems. In parallel, N, Chl and ribulose-bisphosphate carboxylase-oxygenase (Rubisco) content was measured from the same leaves. The amount of N in photosynthetic proteins was calculated from the measured contents of the components of the photosynthetic machinery. Non-photosynthetic N was found as the residual of the budget. Growth in shade resulted in the decrease of leaf dry mass to a half of the DW in sun leaves in each species, but the total variation, from the top to the bottom of the canopy, was larger. Through the whole cross-section of the canopy, leaf dry weight (DW) and Rubisco content per area decreased by a factor of four, N content by a factor of three, but Chl content only by a factor of 1.7. PSII density decreased by a factor of 1.9, but PSI density by a factor of 3.2. The density of PSI adjusted to shade to a greater extent than the density of PSII. In shade, the distribution of N between the components of the photosynthetic machinery was shifted toward light-harvesting proteins at the expense of Rubisco. Non-photosynthetic N decreased the most substantially, from 54% in the sun leaves of *B. pendula* to 11% in the shade leaves of *T. cordata*. It is concluded that the redistribution of N toward light-harvesting Chl proteins in shade is not sufficient to keep the excitation rate of a PSII centre invariant. Contrary to PSII, the density of PSI – the photosystem that is in immediate contact with the carbon assimilation system – shade-adjusts almost proportionally with the latter, whereas its Chl antenna correspondingly increases. Even under N deficiency, a likely condition in the natural plant community, a substantial part of N is stored in non-photosynthetic proteins under abundant irradiation, but much less under limiting irradiation. At least in trees the general sequence of down-regulation due to shade adjustment is the following: (1) non-protein cell structures and non-photosynthetic proteins; (2) carbon assimilation proteins; (3) light reaction centre proteins, first PSI; and (4) chlorophyll-binding proteins.

Key-words: nitrogen; photosystems; Rubisco; sun–shade adjustment.

Abbreviations: Cyt b_6f, cytochrome b_6f; Cyt f, cytochrome f; J, electron transport rate; F_0, F_s, F_m, fluorescence yields, minimum, steady state, maximum (all in the light), respectively; FRL, far-red light; LHC, light-harvesting complex; P_s, P_m, P_o, P700 reduction, steady-state, maximum and corresponding to pulse-oxidizable P700; PC, plastocyanin; PSI, PSII, photosystems I and II; PQ, plastoquinone; P700, donor pigment of PSI; Rubisco, ribulose 1,5-bisphosphate carboxylase-oxygenase; SAC, shade adjustment coefficient; TSF, total site factor, characterizes relative irradiance at the site; WL, white light; Y_C, Y_F, Y_P, quantum yields of photosynthetic e^- transport, calculated from CO_2 uptake, Chl fluorescence and 820 nm transmission, respectively; other, definitions in legend to Table 1.

INTRODUCTION

In a canopy, a plant's photosynthetic machinery adjusts toward the optimal proportions of light and dark reactions. The light reactions comprise the two photosystems II and I (PSII and PSI), and of the e^- transport chain, while the dark reactions comprise of the CO_2 fixation and reduction chemistry that is linked to the CO_2 diffusion pathway. Quite evidently, in upper, sun leaves of the canopy the optimum requires a greater capacity of the dark reactions, whereas in lower, shade leaves the light-capturing system is more important. Since the development of the whole machinery is based on the availability of N, which is usually limiting in natural canopies, the optimal distribution of N between the constituents of the light and dark reactions is

Correspondence: A. Laisk. Fax: +372 7420286; e-mail: Agu.Laisk@ut.ee

Table 1. Photosynthetic parameters of sun and shade leaves

	B. pendula			*T. cordata*			*S. virgaurea*		
Parameter	Sun	Shade	SAC	Sun	Shade	SAC	Sun	Shade	SAC
Rel. irradiance, TSF	0.86 ± 0.3	0.17 ± 0.02	**0.80**	0.28 ± 0.05	0.15 ± 0.01	**0.46**	0.63 ± 0.01	0.13 ± 0.01	**0.79**
FW g m^{-2}	210 ± 9.7	125 ± 9.0	**0.40**	128 ± 3.3	83 ± 2.5	**0.35**	161 ± 11.7	94 ± 4.8	**0.42**
DW g m^{-2}	87 ± 3.3	46 ± 2.9	**0.47**	48 ± 1.4	25 ± 0.7	**0.49**	44 ± 3.6	21 ± 0.6	**0.52**
TotProtein g m^{-2}	8.46 ± 0.64	4.85 ± 0.28	**0.43**	5.44 ± 0.31	2.90 ± 0.11	**0.47**	6.92 ± 0.91	2.86 ± 0.19	**0.59**
SolProtein g m^{-2}	7.6 ± 0.4	4.8 ± 0.2	**0.37**	4.7 ± 0.2	2.6 ± 0.2	**0.45**	4.6 ± 0.7	1.8 ± 0.2	**0.61**
RBC site μmol m^{-2}	37 ± 2	20 ± 2	**0.44**	22 ± 2	12 ± 1	**0.45**	23 ± 5	10 ± 1	**0.59**
Chl μmol m^{-2}	525 ± 24	426 ± 16	**0.19**	469 ± 33	440 ± 32	0.06	516 ± 113	317 ± 22	0.38
Chl/RBC site	14.7 ± 1.2	21.3 ± 1.4	**–0.45**	22.4 ± 2.7	37.9 ± 4.4	**–0.69**	22.4 ± 2.2	33.7 ± 3.3	**–0.50**
Chl *a*/*b*	3.826 ± 0.068	3.396 ± 0.066	**0.11**	3.378 ± 0.097	3.008 ± 0.037	**0.11**	3.159 ± 0.129	3.098 ± 0.062	0.02
a_{II}	0.457 ± 0.013	0.486 ± 0.006	**–0.06**	0.467 ± 0.009	0.463 ± 0.015	0.01	0.461 ± 0.008	0.477 ± 0.005	–0.03
a_I	0.449 ± 0.015	0.476 ± 0.004	–0.06	0.522 ± 0.009	0.489 ± 0.019	0.06	0.470 ± 0.015	0.482 ± 0.016	–0.03
N_{II} μmol m^{-2}	1.33 ± 0.07	0.97 ± 0.04	**0.27**	1.12 ± 0.15	1.06 ± 0.09	0.05	0.94 ± 0.16	0.68 ± 0.07	**0.28**
N_I μmol m^{-2}	1.23 ± 0.06	0.77 ± 0.05	**0.38**	0.71 ± 0.05	0.53 ± 0.03	**0.25**	0.74 ± 0.09	0.38 ± 0.03	**0.49**
PC_rel	1.87 ± 0.05	1.92 ± 0.02	–0.02	1.99 ± 0.09	1.73 ± 0.15	0.13	1.57 ± 0.15	1.86 ± 0.11	–0.18
Cyt_rel	1.04 ± 0.10	0.80 ± 0.04	0.23	1.21 ± 0.10	1.00 ± 0.02	0.17	0.96 ± 0.13	0.72 ± 0.07	0.25
PSUII	183 ± 10	221 ± 15	**–0.21**	200 ± 16	206 ± 9	–0.03	249 ± 21	232 ± 10	0.07
PSUI	192 ± 9	275 ± 14	**–0.43**	342 ± 46	414 ± 48	–0.21	315 ± 43	400 ± 15	–0.27
PQ μmol e^- m^{-2}	27.8 ± 1.2	15.2 ± 0.5	**0.45**	8.1 ± 1.7	4.3 ± 1.7	**0.47**	11.8 ± 1.8	n.m.	

Rel. irradiance, total site factor; FW, fresh weight; DW, dry weight; TotProtein, total protein calculated on the basis of N content; SolProtein, soluble protein; RBC site, area density of Rubisco active sites; Chl, area density of chlorophyll; Chl *a*/*b*, chl *a*/*b* ratio; a_{II}, a_I, relative optical cross-section of PSII and PSI antenna; N_{II}, N_I, area density of photosystems II and I; PC_rel, Cyt_rel, relative abundance of plastocyanin and cytochrome f in relation to PSI; PSU II and PSU I, total antenna size (photosynthetic unit) of PSII and PSI; PQ, plastoquinone (μmol e^- m^{-2}, 2 e^- per PQ). SAC, shade adjustment coefficient (statistically significant presence of shade adjustment indicated in bold).

of crucial importance for an efficient photosynthetic performance.

The importance of nitrogen content and distribution in leaves, as the substance of photosynthetic enzymes, was addressed by Evans (1983a, b; reviewed: 1989). In many plant species photosynthetic rate at high irradiance was found to be proportional to the N content of leaves (Kull & Jarvis 1995; Woodward, Smith & Emanuel 1995; Friend *et al*. 1997). Despite the fact that the proportionality factor varied substantially in different species (Evans 1989; Reich, Walters & Ellsworth 1997; Kull 2002) a working hypothesis was proposed that, in case of complete adjustment to shade, N content per area, in the leaves of a canopy should follow the average irradiance profile in the canopy (Field 1983; Kull & Jarvis 1995; Kull 2002; Meir *et al*. 2002). However, although such adaptation does occur, it is variable and not complete: the N content (and the corresponding capacity of the photosynthetic machinery) in the lowest leaves of a canopy is greater than necessary to handle the average irradiation at the bottom of the canopy (Meir *et al*. 2002).

This variability in the photosynthesis versus N relationship may have several causes. First, not all N in the leaf is in the photosynthetic machinery. This is particularly clear in fertilization experiments or hydroponic cultures with a high level of N, when inorganic N content in leaves may be built up (Evans & Poorter 2001; Lawlor 2002), but has also been observed in plants growing in natural habitats, where N is usually limiting, since estimates of the photosynthetic N fraction reveal a substantial residual, non-photosynthetic N fraction (Evans 1989; Frak *et al*. 2001; Gonzalez-Real & Baille 2000).

Second, along with the decreasing N content per area in the leaves of the lower layers of the canopy, there also occurs a redistribution of N between partial processes of photosynthesis. In the upper layers of the canopy, light is in excess and N is preferentially used to build up an efficient machinery for CO_2 fixation and carbon metabolism. In the lower levels of the canopy, light is limiting and more N is distributed to Chl-protein complexes for efficient light capture (Evans & Terashima 1987; Terashima & Evans 1988; Hikosaka & Terashima 1996; reviewed: Anderson & Osmond 1987; Evans 1989). Similar acclimation in the photosynthetic apparatus in response to an irradiance gradient occurs also on the chloroplast level within a leaf (Laisk & Oja 1976; Terashima 1989; Nishio, Sun & Vogelmann 1993; Terashima & Hikosaka 1995; Evans 1995).

Third, the paradigm of N-based photosynthetic machinery assumes that N-containing enzymes are fully active. Evidence shows that the most important photosynthetic enzyme Rubisco may not be fully active in naturally growing leaves (Eichelmann & Laisk 1999; Eichelmann *et al*. 2004a) and that the enzyme protein may be used partially as a N storage (Theobald *et al*. 1998; Warren, Adams & Chen 2000).

The vast majority of studies on photosynthetic acclimation within tree canopies deal only with a few basic photosynthetic parameters, trying to parameterize popular models (Farquhar, von Caemmerer & Berry 1980; Ellsworth & Reich 1993; Brooks, Sprugel & Hinckley 1996; Hollinger 1996; Dang *et al*. 1997; Niinemets, Kull & Ten-

hunen 1998; Le Roux, Sinoquet & Vandame 1999; Bond *et al*. 1999; Meir *et al*. 2002). On the other hand, it is well known from detailed laboratory studies that the acclimation of photosynthesis to irradiation involves several changes in the stoichiometry of the components of the photosynthetic apparatus (Anderson, Chow & Park 1995). Such changes are usually not documented in field studies, mostly due to technical difficulties in the methods and artefacts introduced by destructive laboratory techniques. Recently, a routine of non-destructive gas exchange and optical measurements was reported, which makes it possible to obtain information about the components of the photosynthetic machinery (Laisk *et al*. 2002). We have applied these methods to investigate changes in the photosynthetic machinery in developing birch leaves (Eichelmann *et al*. 2004a) and in birch leaves growing under conditions of elevated CO_2 and O_3 (Eichelmann *et al*. 2004b). In this work we have addressed the adjustment of the light reactions, particularly the size of the Chl antenna of the photosystems, to low light in leaves of different species extending through a gradient of irradiation in a canopy. The species were chosen by their different sun and shade acclimation capacity. A rather limited redistribution of N between the components of the light and dark photosynthesis reactions was observed.

MATERIALS AND METHODS

Study site and plant material

Plant material was collected in July 2002 in a mixed deciduous forest stand in Järvselja, Estonia (58°22′ N, 27°20′ E). Two tree species, *Betula pendula* Roth and *Tilia cordata* P. Mill. and a herbaceous species *Solidago virgaurea* L. were chosen for the study according to their shade tolerance and acclimation ability, known from our previous studies. *Betula pendula*, a typical light-demanding tree, is an overstorey species with a height of 10–27 m; *T. cordata*, a typical shade-tolerant tree, is a subcanopy species (4–17 m). *Solidago virgaurea* was chosen for comparison as an herbaceous species with a wide ecological amplitude, growing naturally under the tree canopy as well as on open clearings. The small size of *S. virgaurea* allowed the excavation of entire plants and leaves to be kept intact during transportation to the laboratory and the measurements. Shoots of the trees and individuals of the herb were taken from either end of their occurrence along the natural gradient of irradiance. Tree shoots were taken from the tops of the trees, the most illuminated locations and from the lowest branches, the most shaded locations. *Solidago virgaurea* plants were taken from the most shaded understorey and from the open clearing nearby. Every growth site was represented by five samples, from which averages and standard errors were calculated.

Radiation environment

Light conditions at every sampling point were estimated as total site factor (TSF) using the hemispherical photography system SCANOPY PRO (Scanopy Pro Regent Instruments, Sainte-Foy, Quebec, Canada). A digital photo was taken from every sampling location with a Nikon CoolPix 900 camera (Nikon Corporation, Tokyo, Japan) equipped with a hemispheric converter. Images were processed for estimates of canopy gap distribution and TSF using both colour and brightness information by SCANOPY PRO software. TSF equals fractional irradiance on the horizontal plane when irradiance above the canopy equals 1. Independent of the actual TSF value, we shall denote as 'sun' and 'shade' the leaves sampled from the most and least illuminated sites, respectively, although the extreme TSF values differed by about five times for *B. pendula*, but only about two times for *T. cordata*.

Photosynthetic characteristics

Shoots were cut from the plant and immediately immersed in water or an individual *S. virgaurea* plant was excavated and kept in watered soil. After about 2 h (in some cases overnight, 8–10 h) of dark adaptation, a leaf attached to the shoot (or plant), was fitted to the leaf chamber of the gas system in the laboratory and a routine of gas exchange and optical measurements was applied with the aim of diagnosing the photosynthetic machinery. Sufficient stomatal conductance during the measurements was taken as the criterion for intactness of the excised shoot. A few shade leaves of *T. cordata* were rejected on this basis.

The leaf chamber had a diameter of 31 mm, height 3 mm; the gas flow rate was 0.5 mmol s^{-1}. The combined gas-exchange/optical system allowed the operator to vary incident quantum flux densities and chamber CO_2 and O_2 concentrations almost immediately, and to record CO_2 uptake, O_2 evolution, Chl fluorescence, and 820 nm absorptance, for non-intrusive characterization of the partial reactions of photosynthesis (Laisk *et al*. 2002; Eichelmann *et al*. 2004a). CO_2 exchange was measured with an infrared CO_2 analyser LI-6251 (LiCor, Inc., Lincoln, NE, USA), and O_2 evolution with a zirconium electrode analyser S-3 A (Ametek, Pittsburgh, PA, USA). The leaf chamber was illuminated through a multi-arm light guide from three Schott KL 1500 sources (Schott GmbH, Mainz, Germany), providing actinic white light (WL), fluorescence saturation pulses of white light of 11 000 μmol m^{-2} s^{-1} (2.5 s), and far-red light (FRL) centred at 720 nm (an interference filter from Andover Corp., Salem, NH, USA, spectra see Oja *et al*. 2003). Incident quantum flux density was measured with a quantum sensor (LI-190SA; LiCor, Inc.). Leaf absorptance was determined for WL and FRL in an Ulbricht-type integrating sphere using a spectroradiometer PC-2000 (Ocean Optics, Dunedin, FL, USA). Chlorophyll fluorescence variables for characterization of PSII activity were measured with a pulse-modulated fluorometer PAM-101 and an emitter-detector unit 101ED, equipped with a short-pass filter for protection against simultaneous 820 nm pulsing (H. Waltz GmbH, Effeltrich, Germany). PSI activity was characterized by leaf transmittance measurements with another PAM-101 fluorometer along with the emitter-detector unit ED P700DW (H. Walz GmbH, remanufactured for wave-

length difference 810–950 nm). The output signal of this device reflects the presence of $P700^+$ and plastocyanin (PC^+) and is termed the 'P700DW signal' below.

Properties of the light reactions of photosynthesis were determined as described earlier (Laisk *et al*. 2002) and will briefly be described below, as well as the changes introduced by deconvolution of the P700DW signal into $P700^+$ and PC^+ components (Oja *et al*. 2003).

Relative antenna cross-sections of PSII and PSI

The measurement of the relative antenna cross-section (quantum partitioning ratio) was based on the analysis of e^- flow rates through the photosystems at very low irradiance. Photosynthetic CO_2 fixation rate was measured under strictly limiting irradiances of 15, 35 and 70 μmol quanta m^{-2} s^{-1} under air levels of CO_2 and O_2 (360 μmol CO_2 mol^{-1} and 210 mmol O_2 mol^{-1}); the rate of linear electron transport associated with the photosynthetic carbon metabolism (J_C) was calculated considering RuBP carboxylation and oxygenation (Laisk & Loreto 1996; Peterson, Oja & Laisk 2001) and the quantum yield of this e^- transport was calculated for the above light intensities as

$$Y_C = \frac{J_C}{I} = \frac{4(A_n + R_K)}{I}\frac{2K_sC_c + 2O_c}{2K_sC_c - O_c} \quad (1)$$

where I is absorbed photosynthetic quantum fluence rate, A_n is the measured net rate of CO_2 assimilation, R_K is the rate of dark respiration in the light, K_s is the CO_2/O_2 specificity factor for Rubisco, C_c is CO_2 and O_c is the dissolved O_2 concentration at the site of carboxylation. K_s was found from the oxygen dependence of the CO_2 compensation point and R_K in the light was calculated such that the light dependence of Y_C became linear (i.e. the Kok effect was considered; Laisk *et al*. 2002). On the other hand, PSII quantum yield Y_F and PSII e^- transport rate J_F were calculated from Chl fluorescence as

$$Y_F = \frac{F_m - F_s}{F_m} \quad (2)$$

$$J_F = a_{II} I Y_F \quad (3)$$

where F_s is the steady and F_m the maximum (pulse-saturated) fluorescence yield in the light, J_F is e^- flow rate in μmol e^- m^{-2} s^{-1} and a_{II} is the relative optical cross-section of PSII. The proportion of the total absorbed quantum fluence rate that had to be absorbed by PSII in order to support this e^- fluence rate (a_{II}) was found considering the actual quantum efficiency of excitation use by PSII (Laisk & Loreto 1996):

$$a_{II} = \frac{Y_C}{Y_F}. \quad (4)$$

The relative absorption cross-section of PSI, a_I, was determined on a similar principle as that of PSII, but using 820 nm transmittance measurements for determining the actual quantum efficiency of PSI electron transport (Eichelmann & Laisk 2000):

$$a_I = \frac{Y_C}{Y_P}, \quad (5)$$

$$Y_P = \frac{P_o - P_s}{P_m}, \quad (6)$$

where P_m is the signal corresponding to totally oxidized P700 (full P700 pool), P_o is the pulse-oxidizable fraction and P_s is the steady-state oxidation signal. Earlier (Eichelmann & Laisk 2000) the whole 820 nm signal was taken to be proportional to $P700^+$, but in the present work we deconvoluted the P700DW output signal into $P700^+$ and PC^+ components using the oxidative titration method (Oja *et al*. 2003), so that P in Eqn 6 is the true relative level of un-oxidized P700. The pulse-oxidizable fraction of P700, P_o was measured during a 10-ms saturation pulse of 11 000 μmol quanta m^{-2} s^{-1} (Klughammer & Schreiber 1994).

Chl was assumed to be distributed between photosystems proportionally to a_{II}/a_I.

Plastoquinone, cytochrome b_6f and plastocyanin pools of the electron transport chain

These pools were determined in intact leaves using kinetic methods. The plastoquinone pool was measured as an initial short O_2 evolution burst after a sudden illumination of a dark-adapted leaf (Laisk *et al*. 2002). ATP synthase and CO_2 fixation enzymes were inactivated during a 15-min dark adaptation and only PQ (plus some PSI acceptor side carriers) served as an e^- acceptor during the first few seconds of illumination.

Cyt b_6f and PC pools were determined from the oxidative titration of PSI donor side e^- carriers by FRL (Oja *et al*. 2003). Electrons were accumulated in the PSI donor side carriers in the dark, and the carriers were re-oxidized under FRL. The recorded P700 DW signal transient was mathematically modelled assuming redox equilibrium between P700, PC and Cyt f, considering that $P700^+$ and PC^+ were the signal sources. Relative pool sizes, Cyt f per PSI and PC per PSI, were obtained as best-fit model parameters.

Densities of PSII and PSI

PSII density was determined as four times the O_2 evolution from a saturating single-turnover flash (Oja & Laisk 2000). The flash was applied on top of FRL, which fully oxidized PQ and supported a slow background e^- transport that randomized the s-states of the water-splitting complex.

Two kinetic methods were used for determining PSI density in intact leaves. First, we generated a known amount of e^- from PSII by illuminating the leaf with a saturating single turnover flash and measured, using the P700DW signal, to what extent these e^- reduced the preoxidized PSI donor side (Oja *et al*. 2004). Second, we measured the speed of reduction of $P700^+$ by a known photosynthetic e^- transport rate (Laisk *et al*. 2002). Considering the importance of the PSI density data, the methods will be described in more detail below.

Finally, knowing the distribution of Chl between the photosystems and the densities of the photosystems, N_{II} and N_I, the antenna sizes (photosynthetic units PSUII and PSUI) were calculated as

$$\mathrm{PSUI} = \frac{a_I}{a_I + a_{II}} \cdot Chl / N_I \quad (7)$$

$$\mathrm{PSUII} = \frac{a_{II}}{a_I + a_{II}} \cdot Chl / N_{II} \quad (8)$$

Dry mass, chlorophyll, protein and Rubisco content

A disc of 1.86 cm^2 was excised from the part of the leaf that had been enclosed in the gas-exchange chamber. The disc was ground in liquid nitrogen, and homogenized in 0.8 mL of 50 mM MES-NaOH buffer (pH = 6.8) that contained 20 mM $MgCl_2$, 50 mM 2-mercaptoethanol and 1% (w/w) Tween-80 (all reactives from Sigma-Aldrich Corp., St. Louis, MO, USA). Two hundred microlitres of this homogenate was mixed with 2.8 mL 80% (v/v) acetone, the mixture was vortexed and kept overnight at 4 °C in the dark, then centrifuged at 12 000 *g* for 10 min. Chlorophyll *a* and *b* content in the supernatant were measured according to Vernon (1960).

The rest of the homogenate was centrifuged at 12 000 *g* for 10 min and soluble protein was precipitated from 200 μL of the supernatant with 0.5 mL 96% (v/v) ethanol. After centrifugation for 10 min at 12 000 *g* the sediment was dissolved in 0.1 M NaOH and the protein content was estimated according to Bradford (1976) using human serum albumin as a standard.

One hundred microlitres of the homogenate was diluted with a sodium dodecyl sulphate- polyacrylamide gel electrophoresis loading buffer and kept at –30 °C until the electrophoresis. The gels were stained with Coomassie blue and the optical density of the Rubisco large subunit band was integrated using Bio-Rad MULTI-ANALYST software (Hercules, CA, USA) and spinach Rubisco as a standard (the Rubisco large subunit protein accounted for 47% of the total protein in the standard preparation). The total mass of Rubisco protein in samples was calculated assuming that the large subunit comprises 80% of the total Rubisco protein, and the number of active sites was calculated assuming the molecular mass of 550 000 g mol^{-1} and eight active sites per molecule.

The fresh weight (FW) of another leaf disc was measured, then the disc was dried at 70 °C for at least 48 h before dry mass (DW) determination.

Calculation of N distribution

The amount of N in a component of the photosysnthetic machinery was found from its molar area density, considering the molar mass and assuming that the relative N content per mass unit of any protein was 16%. Total N content of leaves was measured by the micro-Kjeldahl method (Kjeltec Auto 1030; Foss Tecator AB, Hoeganaes, Sweden) and non-photosynthetic N was found as the residual of the budget.

The mass of N in the PSII core (psbA – psbT) was calculated from the measured PSII density N_{II} (μmol m^{-2}) using the total molar mass of 333.5 kDa (J. Barber, http://www.bio.ic.ac.uk/research/Barber/). Similarly, the amount of N in the PSI core (psaA – psaM) was calculated from the measured PSI density N_I using the molar mass of 290 kDa (Buchanan, Gruissem & Jones 2000). The number of Chls bound to the PSII core was taken as 54 (50 in CP43 + CP47 and 4 in D1 + D2); the number of Chls in the PSI core was taken as 98 (Buchanan *et al*. 2000). Total Chl was assumed to be distributed between the photosystems in proportion with the measured optical cross-sections a_{II} and a_I. The Chl associated with PSII and PSI was calculated separately and the Chl associated with the core of the photosystem was subtracted from the total Chl associated with the particular photosystem. The rest of the Chl was assumed to be bound to the LHC protein. Although there are several Chl-proteins associated with PSI (lhca1 – lhca4) and PSII (lhcb1 – lhcb6), we assumed an average molar mass of 2 kDa of protein per Chl. The N associated with the LHC protein was calculated considering this ratio, plus the N of Chl itself (it was also considered in the calculation of the N of the PSII and PSI core).

The amount of N in Rubisco was calculated directly from the measured Rubisco content. The amount of N in the Cyt b_6f complex was calculated from the measured PSI density and the measured Cyt/PSI ratio, taking the molar mass of Cyt b_6f to be 103 kDa (Buchanan *et al*. 2000). The amount of N in the ATP synthase was calculated assuming 1.2 ATP synthases per PSI, taking the molar mass of the CF0 – CF1 complex to be equal to 554 kDa (Buchanan *et al*. 2000). The fractions of N were calculated separately in the core and in the LHC of the photosystems, in the Cyt b_6f, ATP synthase, and Rubisco. The residual of the N budget was assumed to be non-photosynthetic.

Shade adjustment

Shade adjustment of different parameters was characterized by the shade adjustment coefficient SAC, calculated as

$$SAC = 1 - \frac{Shade}{Sun} \quad (9)$$

where *Shade* and *Sun* are respective measured values in shade and sun leaves. SAC increases with more extensive adjustment, it is positive when the shade value is smaller than the sun value.

RESULTS

Determination of PSI density

We used two methods for non-intrusive determination of PSI density. In the first method, we generated a known number of e^- from PSII, measured as $4 \times O_2$ evolution, and optically measured to what extent these e^- reduced preox-

idized P700 (Oja *et al*. 2004). The donor side of PSI was oxidized under FRL, a saturating single turnover flash of WL was applied and FRL was turned off simultaneously. The amount of O_2 that evolved following the flash was integrated and used for the calculation of PSII density N_{II}, as well as the calculation of the number of e^- generated from PSII (Oja & Laisk 2000). The recording of the P700DW signal following the flash, converted into the number of e^- per PSI, is shown in Fig. 1. A sharp deflection toward oxidation was recorded immediately after the flash (the steady state under FRL was defined as zero e^-/PSI, but the true full oxidation level was achieved only after the flash). During the initial fast phase of reduction (< 100 ms) the PSII e^- arrived at PSI, but the fast reduction was followed by a slow spontaneous reduction of the interphotosystem chain by e^- coming from stromal reductants. This spontaneous reduction was reproduced as a reference line in another measurement without the flash. The difference between the two traces reflects e^- that arrived from PSII. In this particular experiment the number of e^- generated by the flash was 1.14 μmol e^- m^{-2}. These e^- made up 0.92 e^- per PSI, as seen from the difference between the full oxidation (–0.33 e^-/PSI) and the reduction state achieved due to the PSII e^- only (0.59 e^-/PSI). From these data, PSI density, N_I, was 1.14/0.92 = 1.24 μmol m^{-2}. The PSI density obtained this way varied from 1.2 in sun to 0.4 μmol m^{-2} in shade leaves and was subject to significant shade adjustment (Table 1).

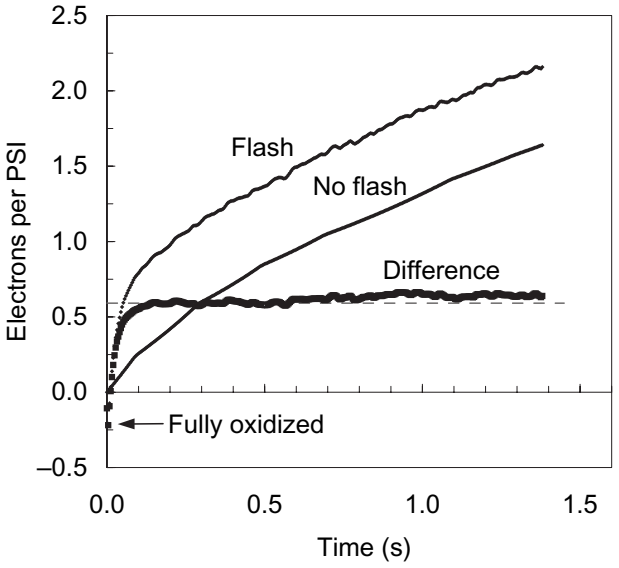

Figure 1. Reductive titration of PSI density by electrons from PSII. A sun leaf of *B. pendula* was exposed under FRL and a saturating single-turnover flash was applied. The number of electrons generated by PSII was measured as O_2 evolution. The flash fully oxidized P700, but then electrons arriving from PSII rapidly reduced the PSI donor side carriers $P700^+$ and PC^+ (first 100 ms), followed by slower spontaneous electron arrival from stromal reductants. The latter process was recorded as a reference without the flash, and the difference showed the reductive effect of flash-generated PSII electrons only. The ordinate is calibrated in e^- per PSI, calculated by deconvoluting the P700DW signal into PC^+ and $P700^+$ components (Oja *et al*. 2003). PSI density was calculated knowing the number of electrons and the degree to which they reduced $P700^+$ (Oja *et al*. 2004).

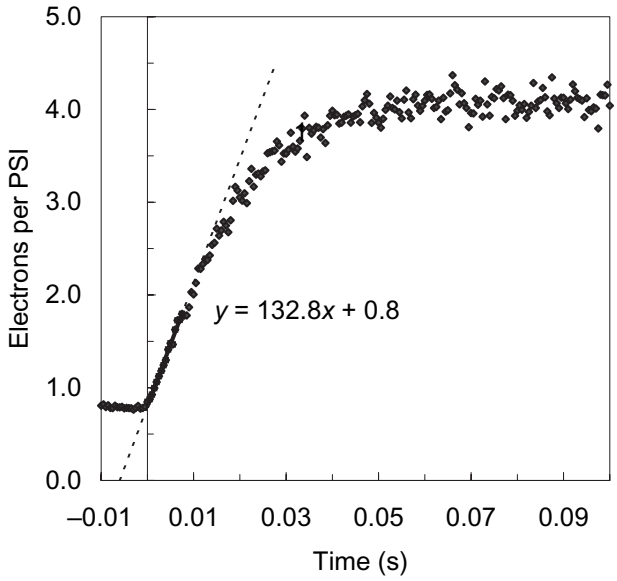

Figure 2. Determination of PSI density from the speed of $P700^+$ reduction. Steady-state photosynthesis under strong saturating irradiance was interrupted by darkening and the speed of reduction of $P700^+$, k_I, was recorded and deconvoluted as the number of e^- per PSI s^{-1}. Electron transport rate J_F was calculated from fluorescence measurements (Eqn 3) and PSI density was found from the speed of P700 reduction as $N_I = J_F/k_I$ (Laisk *et al*. 2002).

The second method for PSI determination was based on the measurement of how fast a known photosynthetic e^- transport rate (μmol e^- m^{-2} s^{-1}) reduces the pre-oxidized PSI donor side (e^-/PSI per s). The ratio of the two quantities gives us PSI density (μmol PSI m^{-2}). This method has been applied before (Laisk *et al*. 2002; Eichelmann *et al*. 2004b), but in the present work we converted the P700DW signal into e^-/PSI using the oxidative titration method (Oja *et al*. 2003).

Light-saturated, steady-state photosynthesis was interrupted by sudden darkening and the light–dark transient of the P700DW signal was recorded. The steady-state PSII e^- transport rate J_F was 162 μmol e^- m^{-2} s^{-1} in this leaf, as determined from Chl fluorescence measurements (Eqn 3). At a high irradiation density the PSI donor side was partially oxidized, since there were 0.78 e^-/PSI in this birch leaf at the high irradiance (Fig. 2). After the sudden darkening, the number of e^-/PSI increased at the PSI donor side, at first linearly in time, but then slowing and saturating later at 4.1 e^-/PSI (of which one was in P700 and, on average, two in PC and one in Cyt f). The initial slope of the trace shows the speed of e^- arrival at PSI, equivalent to the steady-state rate of PSI turnover immediately before the light was interrupted (k_I = 133 e^-/PSI s^{-1} in this leaf). Assuming that e^- transport rate through PSI, $J_I = J_F$ and is expressed as $J_I = k_I N_I$, where N_I is PSI density, μmol m^{-2}, and k_I is the turnover rate of PSI, s^{-1}, we obtain $N_I = J_F/k_I$ = 162/133

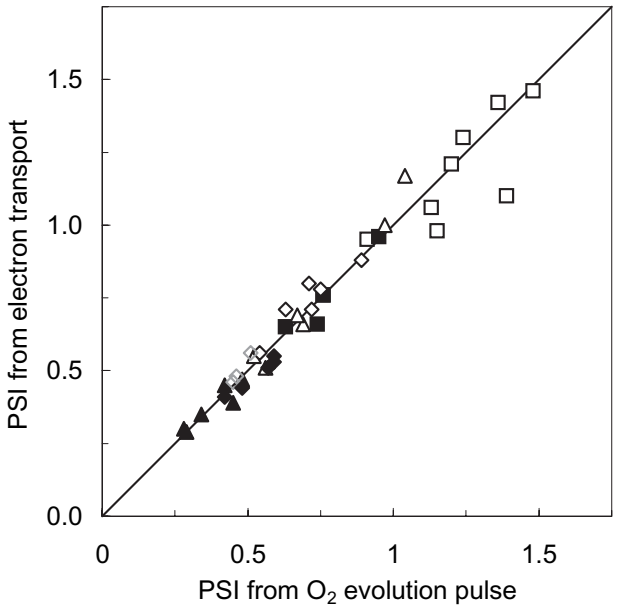

Figure 3. Comparison of PSI densities determined from the reductive titration (O_2 evolution measurements, abscissa) and from the speed of dark re-reduction of P700 under the influence of photosynthetic electron transport (ordinate). Squares, *B. pendula*; diamonds *T. cordata*; triangles, *S. virgaurea*. Open symbols, sun, closed symbols, shade leaves.

= 1.22 μmol m^{-2}. The experiment was repeated on the same leaf at different J_F values obtained under different irradiances, and the resulting PSI densities scattered only by a few percent. Over all leaves, the correlation between the two methods was excellent (Fig. 3). Since the e$^-$ transport method was based on an assumption that e$^-$ transport rates through both photosystems were equal, the good 1 : 1 proportionality of the results also shows that there was little cyclic e$^-$ flow around PSI on top of the linear e$^-$ flow. Comparison of the densities of the two photosystems shows that there was no fixed stoichiometry; PSII density was either equal or higher than PSI density (Fig. 4).

Shade adjustment

The DW was considerably smaller in shade than in sun leaves (Table 1). Interestingly, the relative shade adjustment coefficient (SAC) of DW was a quite similar 0.5 ± 0.03 in all species. The percentage of N in DW varied relatively little. Total protein was calculated on the basis of the measured N content, assuming that there was very little non-proteinous N in the leaves, and it made up about 13% of DW in trees and 16% in *S. virgaurea*. The relative content of Rubisco in soluble protein was about 35%; the relative shade adjustment was 0.4–0.5 in trees and 0.6 in *S. virgaurea*, more or less the same in Rubisco, in soluble and total protein.

Contrary to the significant shade adjustment in DW and proteins, the shade adjustment was small (0.1–0.2) but significantly positive in the Chl content of tree leaves, but greater in *S. virgaurea* (0.4 on average, but widely variable). In all cases the Chl content was lower in shade than in sun leaves. The ratio of Chl per Rubisco active site ranged from 14 to 37, being always higher in shade than in sun leaves. A little less than a half of Chl was connected with PSII (a_{II} = 0.46–0.49) and a similar amount with PSI. The distribution of Chl between photosystems did not adjust to shade. On average 1–9% of quanta (but up to 20% in a few individual leaves), were absorbed by photosynthetically inactive chromophores. The presence of the photosynthetically inactive chromophores inevitably decreased the quantum yield of photosynthesis (Fig. 5).

The density of O_2 evolving PSII centres was higher in trees (1–1.3 μmol m^{-2}) and lower in *S. virgaurea* (0.7–0.9 μmol m^{-2}, Table 1). It significantly adjusted to shade in *B. pendula* and *S. virgaurea*, but not in *T. cordata*. The density of photochemically active PSI centres was smaller than PSII density and was subject to stronger shade adjustment than the PSII density. Another constituent characteristic of the thylakoid development, the plastoquinone pool (PQ) also decreased in shade leaves; its SAC was twice that of PSII (0.47 in *B. pendula* and *T. cordata*). Antenna size (photosynthetic unit, PSU) was calculated considering the Chl content, its relative distribution between photosystems and the content of the photosystems (Eqns 10, 11). PSU II was somewhat larger in shade than in sun leaves of *B. pendula*, but did not adjust to shade in *T. cordata* and *S. virgaurea*. PSU I, on the contrary, substantially increased in the shade leaves of all species.

Correlations in individual leaves

Although the leaves were sampled from habitats that were as distinctly sun and shade as possible, their parameters still varied, allowing us to look for correlations between photo-

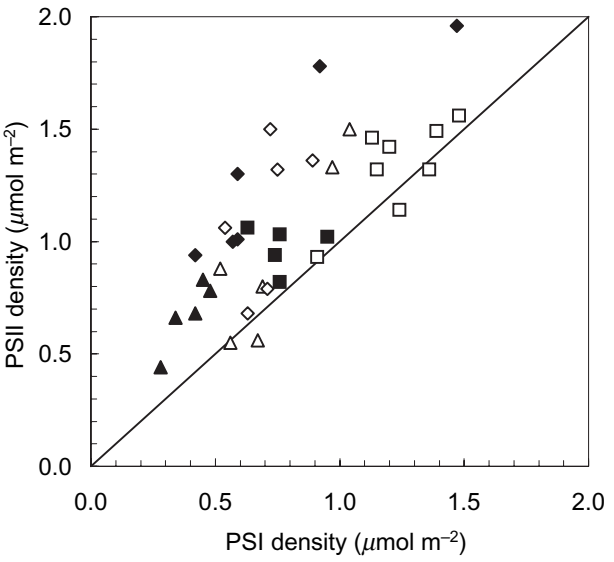

Figure 4. Comparison of PSII and PSI densities. Symbols explained in legend to Fig. 3.

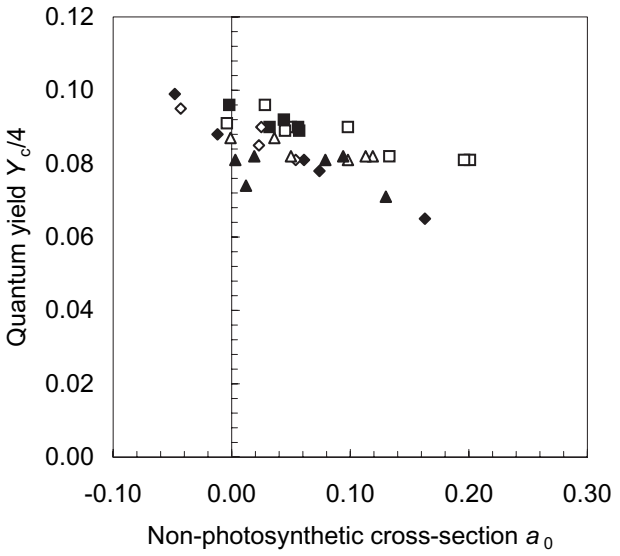

Figure 5. Dependence of the maximum quantum yield of CO_2 fixation under non-photorespiratory conditions $Y_C/4$ on the non-photosynthetic absorption cross section $a_0 = 1 - a_{II} - a_I$. The quantum yield was calculated for e^- transport (Eqn 1). Symbols explained in legend to Fig. 3.

synthetic parameters and protein (N) content in individual leaves. The non-proteinous mass was rather proportionally related to protein, about 8 g per 1 g of protein, although the parameter decreased in deep shade leaves (Fig. 6a). The graph of soluble protein showed an offset, reflecting the relative decrease in soluble stromal photosynthetic and reserve proteins in shade leaves (Fig. 6b). There was weak correlation between Rubisco content and total protein ($R^2 = 0.7$, data not shown), but stronger correlation between the soluble protein and Rubisco (Fig. 6c, $R^2 = 0.83$). Correlation between total protein and PSI was weak (Fig. 6d, $R^2 = 0.7$), but practically absent between total protein and PSII ($R^2 = 0.3$, data not shown).

Sun–shade re-distribution of N in leaves

Figure 7 illustrates the content and distribution of N in sun and shade leaves. The shade adjustment of total N was substantial in all species, but the photosynthetic N adjusted to shade to a lesser extent than the total N, resulting in a strong shade-adjustment of the non-photosynthetic N. Sun–shade re-partitioning of the photosynthetic N between Rubisco (RBC), Cyt b_6f + ATP synthase, PSI core, LHC of PSI, PSII core and LHC of PSII was not very strong, but significant (Fig. 8). In shade, about 15% of photosynthetic N was re-partitioned to light-harvesting proteins at the expense of Rubisco, leaving the fraction of N in Cyt b_6f + ATP synthase almost constant.

DISCUSSION

Light-dependent alteration of the molecular ecosystem of PSII and the stoichiometry of the two photosystems remains one of the most challenging areas of research in light-resource utilization (Osmond *et al*. 1999). In this work we applied new non-destructive kinetic techniques to measure PSII and PSI density and several other components of the light and dark reactions of photosynthesis in leaves of trees *Betula pendula* Roth and *Tilia cordata* P. Mill. and a herb *Solidago virgaurea* L. growing in a natural canopy either in sunlight or shade. We showed clear adjustment to growth irradiation in proteins – constituents of the photosynthetic machinery.

Nitrogen partitioning: photosynthetic and non-photosynthetic

Nitrogen partitioning between the components of the photosynthetic machinery changed with acclimation to different irradiation conditions. Growth in shade resulted in the decrease of the leaf dry mass to a half of the DW in sun leaves in each species, but the total variation in DW, from the top to the bottom of the canopy, was about five-fold, in accordance with earlier results (Niinemets *et al*. 1998). The relative N content in dry mass changed little: there were 8.2 g of other compounds per gram of protein, although in extreme shade the protein content increased slightly (Fig. 6a), as reported earlier (Niinemets *et al*. 1998). As a consequence, the absolute N content per area decreased substantially.

Few studies that have quantified N partitioning into the photosynthetic apparatus have concentrated on the stoichiometry of its constituents and usually have not shown explicitly the amount of non-photosynthetic N (Niinemets & Tenhunen 1997; Warren *et al*. 2000; Evans & Poorter 2001; Frak *et al*. 2002). Our rather unexpected result was the relatively large sun/shade difference in the non-photosynthetic N, especially in the two species growing under the lowest irradiation density. In the shade leaves of *T. cordata* the non-photosynthetic N dropped very low. Since this result was sensitive to the method of calculation of the photosynthetic N, we also performed the calculation according to Hikosaka & Terashima (1996), but the result was similar: in leaves growing in extreme shade (shade leaves of *T. cordata* and *S. virgaurea*) the fraction of non-photosynthetic N decreased significantly. This behaviour is different from *Alocasia macrorrhiza* and *Chenopodium album* (Hikosaka & Terashima 1996) and spinach (Evans 1989), where the relative share of non-photosynthetic N increased with decreasing growth irradiation. Evidently, species may differ by the relative amount of non-photosynthetic N in their leaves, probably dependent on the availability of N. Because the non-photosynthetic N fraction is variable in leaves within the same canopy, estimates of this fraction made from extrapolation of the photosynthesis-N relationship to zero photosynthesis (e.g. Gonzalez-Real & Baille 2000) should be taken with caution.

On the basis of our data we cannot specify in what form the non-photosynthetic N is in the leaf. Dark respiration was not correlated with it, therefore it seems not to

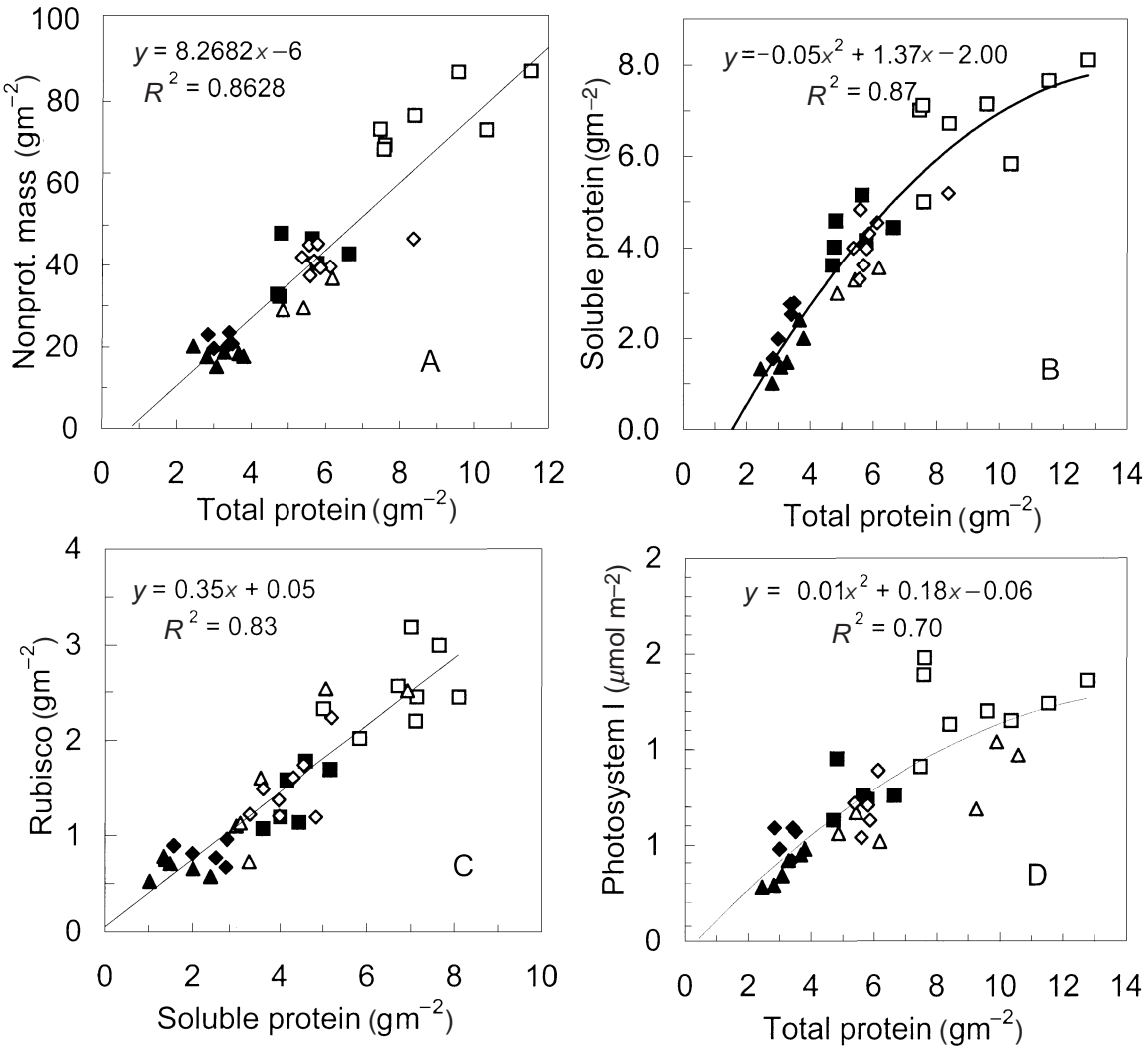

Figure 6. Correlations between the calculated N-based protein content and non-proteinous dry mass (a), soluble protein (b), and photosystem I density (d); Rubisco content is related to soluble protein in (c). Symbols explained in legend to Fig. 3.

be related to the respiratory metabolism (data not shown). Probably the non-photosynthetic N is a kind of reserve concentrated in some metabolically passive proteins. Several studies have shown that, for example, Rubisco may partially serve as a reserve protein in some circumstances, when its average specific activity is low (Theobald *et al*. 1998; Eichelmann & Laisk 1999; Warren *et al*. 2000). Still, in our measurements the non-photosynthetic N cannot be inactive Rubisco, because Rubisco was separately measured and included in the photosynthetic N.

Maybe the fact that *T. cordata* could minimize non-photosynthetic N in its most shaded leaves can be seen as a manifestation of its shade tolerance. The relatively large fraction of non-photosynthetic N in sun leaves shows that, in the presence of abundant energy, N can be accumulated in reserve despite its limited availability in the natural community. Under strictly limiting irradiance the reserve is the first that is deleted from the budget of N.

Nitrogen partitioning within the photosynthetic apparatus

Of the kinetic methods applied in this work, the most critical was the determination of PSI density. For higher reliability we used two methods, which both resulted in well-correlated values (Fig. 3). In a separate work we measured the PSI density in developing birch leaves and found an excellent correlation between the PSI density and leaf optical density at 720 nm, where most of the absorbing Chls are connected with PSI (Eichelmann *et al*. 2004a). The PSII/PSI ratios obtained with our kinetic methods extended from 1 : 1 to 2 : 1 (Fig. 4), in general accordance with earlier reports (Leong & Anderson 1984; Chow, Anderson & Hope 1988; De la Torre & Burkey 1990; Burkey 1993), although somewhat smaller PSII than PSI densities have also been reported (Graan & Ort 1984; Evans & Terashima 1987; Lee & Whitmarsh 1989; Backhausen *et al*. 2000). Quite clearly, the PSII/PSI ratio is not constant, but is

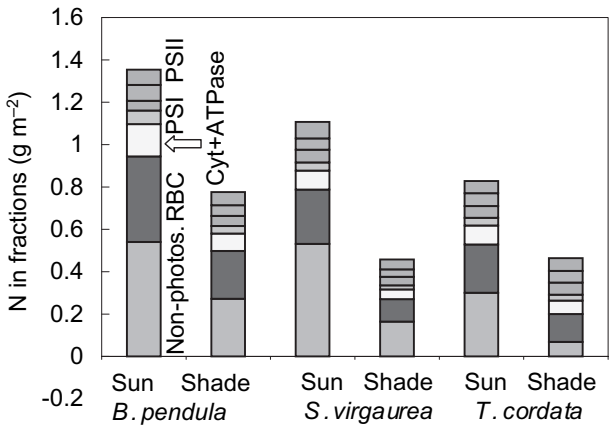

Figure 7. Area-based N content and its allocation to different protein groups in sun and shade leaves. Photosynthetic proteins were calculated as explained in Methods and the non-photosynthetic fraction was found as the residual of the budget. The lower of the two fractions in PSI and PSII is the core, the upper is the light-harvesting Chl proteins.

dependent on leaf age (Eichelmann *et al*. 2004a) and growth conditions (Chow & Hope 1987; Anderson *et al*. 1995).

PSII density significantly decreased in shade in *B. pendula* and *S. virgaurea*, but insignificantly in *T. cordata*. Since *T. cordata* was a sub-canopy species, the contrast between the average growth irradiation for its upper and lower leaves was much smaller than for *B. pendula*, the overstorey species, and *S. virgaurea*, an understorey plant, the samples of which were collected from open and shaded habitats. The result shows that most of the adjustment of PSII density occurs in the range of irradiation density of the upper canopy.

Our kinetic *in vivo* measurements showed a stronger adjustment to shade in PSI density than in PSII density in all studied species and therefore an increasing PSII/PSI ratio with decreasing irradiation. This result is qualitatively consistent with other studies (Anderson & Osmond 1987), but in our measurements PSI density decreased in shade, not only on a leaf area, but also on a Chl basis. Measured as reduced-oxidized extinction difference at 700 nm in thylakoid preparation, the Chl-based PSI density varied relatively little along the irradiation gradient (Anderson & Osmond 1987; Hikosaka & Terashima 1996). In our case the reason for the decrease in PSI density could be the enhancement of PSI excitation by higher FRL in the lower levels of the canopy. Studies with plants grown under manipulated spectral conditions have shown that alterations in the relative rates of excitation of PSI and PSII can lead to changes in photosystem stoichiometry (Chow, Hope & Anderson 1990; Murchie & Horton 1998). However, the ability to shade-adjust the PSI density is also species-dependent, because it was not observed in sunflower, but was observed in tobacco, both grown in the laboratory at high and low irradiance, although PSI was measured by the same techniques as in this work (H. Eichelmann, unpublished).

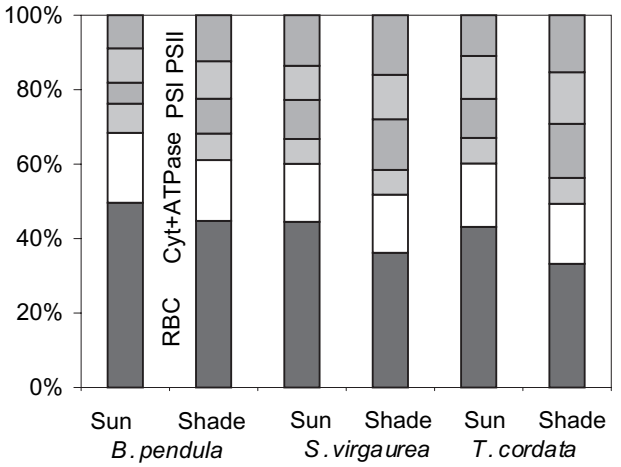

Figure 8. Relative redistribution of N between the photosynthetic proteins in sun and shade leaves. The lower of the two fractions in PSI and PSII is the core, the upper is the light-harvesting Chl proteins.

The distribution of Chl between the two photosystems was calculated proceeding from the necessity of equal excitation rates of the two photosystems. Although the partitioning of excitation does not exactly match the partitioning of Chl (because of the different spectral properties of PSII & PSI Chl Evans 1986), the difference was neglected and Chl was assumed to be shared proportionally to the absorption cross-sections a_{II} and a_{I}. The result showed roughly equal distribution of Chl between the photosystems. Usually less than 10%, but in a few leaves up to 20% of quanta were absorbed by photosynthetically inactive chromophores, such as PSIIβ, plastoquinone non-reducing PSII, and inactive PSI, which decreased the quantum yield of photosynthesis in these leaves (Fig. 5, see also Eichelmann & Laisk 2000).

Knowing the amount and distribution of Chl and the densities of PSII and PSI, the antenna sizes of the photosystems were calculated. In high light the PSII antenna (PSU II) was 183 in *B. pendula*, 200 in *T. cordata* and 249 in *S. virgaurea*. Considering that the PSII core (RC + CP43 + CP47) accommodates 50 Chl and the small peripheral antennae CP29, CP26, and CP24, 14, 14, and 20 Chl, respectively, the core antenna altogether accommodates 98 Chl. If a trimer of LHCII accommodates 39 Chl, then there were on average 2.2, 2.6, and 3.9 LHCII trimers attached to PSII in sun leaves of *B. pendula*, *T. cordata* and *S. virgaurea*, respectively. The number of LHCII trimers increased to 3.2 in the shade-adjusted *B. pendula*, but did not change in the other two species. Contrary to the relatively stable PSII antenna, the PSI antenna was, on average, larger than the PSII antenna and increased by about two LHC trimers due to shade adjustment in all species. This occurred not due to increasing Chl concentration, but due to decreasing PSI density. Other strongly shade-adjusted constituents of the membrane-based photosynthetic machinery were Cyt b_6f and plastoquinone (ATP synthase was assumed to adjust in a stoichiometric 1.3 : 1 ratio with

PSI). Rubisco formed a constant fraction of the soluble protein (Fig. 6c) and its abundance significantly decreased in shade leaves, as expected (Anderson & Osmond 1987; Terashima & Evans 1988; Evans 1989; Hikosaka & Terashima 1996).

The partitioning of N into the light-harvesting constituents clearly increased during the shade adjustment (Fig. 8). Most of the increase in the share of N in the light reactions was in the Chl-binding proteins, which in shade leaves decreased to a lesser extent than other proteins. The relative fraction of N in the PSI core and Cyt b_6f remained constant, whereas the fraction of Rubisco decreased. Thus, the increase in N in the light-harvesting components took place at the expense of Rubisco. However, re-distribution of the photosynthetic N was relatively modest: its total partitioning into light-harvesting constituents increased by 37% and decreased by 32% in Rubisco. Roughly speaking, about 17% of total photosynthetic N was re-partitioned from Rubisco to light-harvesting proteins, although the average irradiance changed by a factor of 2 in *T. cordata* and by 5 in *B. pendula* and *S. virgaurea*.

Thus, the extent of acclimation through balancing energy capture per reaction centre seems to be rather limited. However, this conclusion was obtained from the measurements on whole leaves. Due to self-shading of chloroplasts, a strong gradient of irradiance exists within a leaf and is known to cause chloroplast acclimation (Laisk & Oja 1976; Pearcy 1998; Walters *et al*. 1999). For instance, the gradient of Chl *a*/*b* ratio within a spinach leaf extended from 3.6 at the upper surface to 2.6 in thylakoids close to the lower surface (Terashima 1989), meaning a change in LHCII by at least two trimers, on the basis of the known Chl stoichiometry data (Walters *et al*. 1999). Only about 100 μmol Chl m^{-2} is needed to absorb 60% of incident light. It means that in our leaves that contained about 500 μmol Chl m^{-2}, most of the chloroplasts were still shade-adjusted and only about one-fifth of the photosynthetic apparatus was subject to sun/shade re-adjustment. Thus, it is possible that the actual chloroplast-level sun/shade adjustment range is wider than revealed from our leaf data.

General conclusion

Redistribution of N toward light-harvesting Chl proteins in shade is not sufficient to keep the excitation rate of a PSII centre invariant. Contrary to PSII, the density of PSI, the photosystem that is in immediate contact with the carbon assimilation system, adjusts to shade almost proportionally with the latter, whereas its Chl antenna correspondingly increases. Even under N deficiency, a likely condition in the natural plant community, a substantial part of N is stored in non-photosynthetic proteins under abundant irradiation, but much less under limiting irradiation. At least in trees the general sequence of down-regulation due to shade adjustment is the following: (1) non-protein cell structures and non-photosynthetic proteins; (2) carbon assimilation proteins; (3) light reaction centre proteins, first PSI; and (4) chlorophyll-binding proteins.

ACKNOWLEDGMENTS

This work was supported by the Estonian Ministry of Education and Science and by grants 5466, 5236 and 4584 from Estonian Science Foundation. A.L was supported by a Research Professor grant from Estonian Acad. Sci.

REFERENCES

Anderson J.M. & Osmond C.B. (1987) Shade-sun responses: compromises between acclimation and photoinhibition. In *Photoinhibition* (ed. C.B. Osmond), pp. 1–38. Elsevier. Science Publishers, Amsterdam, The Netherlands.

Anderson J.M., Chow W.S. & Park Y.-I. (1995) The grand design of photosynthesis: acclimation of the photosynthetic apparatus to enviromental cues. *Photosynthesis Research* **46,** 129–139.

Backhausen J.E., Kitzmann C., Horton P. & Scheibe R. (2000) Electron acceptors in isolated spinach chloroplasts act hierarchically to prevent over-reduction and competition for electrons. *Photosynthesis Research* **64,** 1–13.

Bond B.J., Farnsworth B.T., Coulombe R.A. & Winner. W.E. (1999) Foliage physiology and biochemistry in response to light gradients in conifers with varying shade tolerance. *Oecologia* **120,** 183–192.

Bradford M.M. (1976) A rapid and sensitive method for the quantitation of microgram quantities of protein utilizing the principle of protein-dye binding. *Analytical Biochemistry* **72,** 248–254.

Brooks J.R., Sprugel D.G. & Hinckley T.M. (1996) The effects of light acclimation during and after foliage expansion on photosynthesis of *Abies amabilis* foliage within the canopy. *Oecologia* **107,** 21–32.

Buchanan B.B., Gruissem W. & Jones R.L. (2000) *Biochemistry and Molecular Biology of Plants*. American Society of Plant Physiologists, Rockville, MD, USA.

Burkey K.O. (1993) Effect of growth irradiance on plastocyanin levels in barley. *Photosynthesis Research* **36,** 103–110.

Chow W.S. & Hope A.B. (1987) The stoichiometries of supramolecular complexes in thylakoid membranes from spinach chloroplasts. *Australian Journal of Plant Physiology* **14,** 21–28.

Chow W.S., Anderson J.M. & Hope A.B. (1988) Variable stoichiometries of photosystem 2 to photosystem 1 reaction centres. *Photosynthesis Research* **17,** 277–281.

Chow W.S., Hope A.B. & Anderson J.M. (1990) A reassessment of the use of herbicide binding to measure photosystem 2 reaction centres in plant thylakoids. *Photosynthesis Research* **24,** 109–113.

Dang Q.L., Margolis H.A., Sy M., Coyea M.R., Collatz G.J. & Walthall C.L. (1997) Profiles of photosynthetically active radiation, nitrogen and photosynthetic capacity in the boreal forest: implications for scaling from leaf to canopy. *Journal of Geophysical Research* **102,** 845–859.

De la Torre W.R. & Burkey K.O. (1990) Acclimation of barley to changes in light intensity: chlorophyll organization. *Photosynthesis Research* **24,** 117–125.

Eichelmann H. & Laisk A. (1999) Ribulose-1,5-bisphosphate carboxylase/oxygenase content, assimilatory charge and mesophyll conductance in leaves. *Plant Physiology* **119,** 179–189.

Eichelmann H. & Laisk A. (2000) Cooperation of photosystems II and I in leaves as analysed by simultaneous measurements of chlorophyll fluorescence and transmittance at 800 nm. *Plant Cell Physiology* **41,** 138–147.

Eichelmann H., Oja V., Rasulov B., Padu E., Bichele I., Pettai H., Niinemets Ü. & Laisk A. (2004a) Development of leaf photosynthetic parameters in. *Betula pendula* Roth. leaves: correlations with Photosystem I density. *Plant Biology* **6,** 307–318.

Eichelmann H., Oja V., Rasulov B., Padu E., Bichele I., Pettai H.,

Tulva I., Kasparova I., Vapaavuori E. & Laisk A. (2004b) Photosynthetic parameters of birch (*Betula pendula* Roth) leaves growing in normal and in CO_2- and O_3-enriched atmospheres. *Plant, Cell and Environment* **27,** 479–495.

Ellsworth D.S. & Reich P.B. (1993) Canopy structure and vertical patterns of photosynthesis and related leaf traits in a deciduous forest. *Oecologia* **96,** 169–178.

Evans J.R. (1983a) Nitrogen and photosyntesis in the flag leaf of wheat (*Triticum aestivum* L.). *Plant Physiology* **72,** 297–302.

Evans J.R. (1983b) *Photosynthesis and nitrogen partitioning in leaves of Triticum aestivum and related species*. PhD thesis, Department of Environmental Biology, Australian National University, Canberra, Australia.

Evans J.R. (1986) A quantitative analysis of light distribution between the two photosystems, considering variation in both the relative amounts of the chlorophyll-protein complexes and the spectral quality of light. *Photobiochemistry and Photobiophysics* **10,** 135–147.

Evans J.R. (1989) Photosynthesis and nitrogen relationships in leaves of C_3 plants. *Oecologia* **78,** 9–19.

Evans J.R. (1995) Carbon fixation profiles do reflect light absorption profiles in leaves. *Australian Journal of Plant Physiology* **22,** 865–873.

Evans J.R. & Poorter H. (2001) Photosynthetic acclimation of plants to growth irradiance: the relative importance of specific leaf area and nitrogen partitioning in maximizing carbon gain. *Plant, Cell and Environment* **24,** 755–767.

Evans J.R. & Terashima I. (1987) Effects of nitrogen nutrition on electron transport components and photosynthesis in spinach. *Australian Journal of Plant Physiology* **14,** 59–68.

Farquhar G.D., von Caemmerer S. & Berry J.A. (1980) A biochemical model of photosynthetic CO_2 assimilation in leaves of C_3 species. *Planta* **149,** 78–90.

Field C.B. (1983) Allocating leaf nitrogen for the maximisation of carbon gain: leaf age as a control on the allocation program. *Oecologia* **56,** 341–347.

Frak E., Le Roux X., Millard P., Adam B., Dreyer E., Escuit C., Sinoquet H., Vandame M. & Varlet-Grancher C. (2002) Spatial distribution of leaf nitrogen and photosynthetic capacity within the foliage of individual trees: disentangling the effects of local light quality, leaf irradiance, and transpiration. *Journal of Experimental Botany* **53,** 2207–2216.

Frak E., Le Roux X., Millard P., Dreyer E., Jaouen G., Saint-Joanis B. & Wendler R. (2001) Changes in total leaf nitrogen and partitioning of leaf nitrogen drive photosynthetic acclimation to light in fully developed walnut leaves. *Plant. Cell and Environment* **24,** 1279–1288.

Friend A.D., Stevens A.K., Knox R.G. & Cannell M.G.R. (1997) A process-based, terrestrial biosphere model of ecosystem dynamics (Hybrid v3.0). *Ecological Modelling* **95,** 249–287.

Gonzalez-Real M.M. & Baille A. (2000) Changes in leaf photosynthetic parameters with leaf position and nitrogen content within a rose plant canopy (*Rosa hybrida*). *Plant, Cell and Environment* **23,** 351–363.

Graan T. & Ort D.R. (1984) Quantitation of the rapid electron donors to P_{700}, the functional plastoquinone pool, and the ratio of the photosystems in spinach chloroplasts. *Journal of Biological Chemistry* **259,** 14003–14010.

Hikosaka K. & Terashima I. (1996) Nitrogen partitioning among photosynthetic components and its consequence in sun and shade plants. *Functional Ecology* **10,** 335–343.

Hollinger D.Y. (1996) Optimality and nitrogen allocation in a tree canopy. *Tree Physiology* **16,** 627–634.

Klughammer C. & Schreiber U. (1994) An improved method, using saturating light pulses, for the determination of photosystem I quantum yield via $P700^+$-absorbance changes at 830 nm. *Planta* **192,** 261–268.

Kull O. (2002) Acclimation of photosynthesis in canopies. *Oecologia* **133,** 267–279.

Kull O. & Jarvis P.G. (1995) The role of nitrogen in a simple scheme to scale up photosynthesis from leaf to canopy. *Plant, Cell and Environment* **18,** 1174–1182.

Laisk A. & Loreto F. (1996) Determining photosynthetic parameters from leaf CO_2 exchange and chlorophyll fluorescence: Rubisco specificity factor, dark respiration in the light, excitation distribution between photosystems, alternative electron transport and mesophyll diffusion resistance. *Plant Physiology* **110,** 903–912.

Laisk A. & Oja V. (1976) Adaptation of the photosynthetic apparatus to light profile in the leaf. *Fiziologija Rastenij (Soviet Plant Physiology)* **23**, 445–451 (in Russian).

Laisk A., Oja V., Rasulov B., Rämma H., Eichelmann H., Kasparova I., Pettai H., Padu E. & Vapaavuori E. (2002) A computer-operated routine of gas exchange and optical measurements to diagnose photosynthetic apparatus in leaves. *Plant, Cell and Environment* **25,** 923–943.

Lawlor D.W. (2002) Carbon and nitrogen assimilation in relation to yield: mechanisms are the key to understanding production systems. *Journal of Experimental Botany* **53,** 773–787.

Le Roux X., Sinoquet H. & Vandame M. (1999) Spatial distribution of leaf dry weight per area and leaf nitrogen content in relation to local radiation regime within an isolated tree crown. *Tree Physiology* **19,** 181–188.

Lee W.-J. & Whitmarsh J. (1989) Photosynthetic apparatus of pea thylakoid membranes. *Plant Physiology* **89,** 932–940.

Leong T.-Y. & Anderson J.M. (1984) Adaptation of the thylakoid membranes of pea chloroplasts to light intensities. 2. Regulation of electron transport capacities, electron carriers, coupling factor (CF_1) activity and rates of photosynthesis. *Photosynthesis Research* **5,** 117–128.

Meir P., Kruijt B., Broamedow M., Barbosa E., Kull O., Carswell F., Nobre A. & Jarvis P. (2002) Acclimation of photosynthetic capacity to irradiance in tree canopies in relation to leaf nitrogen concentration and leaf mass per unit area. *Plant, Cell and Environment* **25,** 343–357.

Murchie E.H. & Horton P. (1998) Contrasting patterns of photosynthetic acclimation to the light environment are dependent on the differential expression of the responses to altered irradiance and spectral quality. *Plant, Cell and Environment* **21,** 139–148.

Niinemets Ü. & Tenhunen J.D. (1997) A model separating leaf structural and physiological effects on carbon gain along light gradients for the shade-tolerant species *Acer saccharum*. *Plant, Cell and Environment* **20,** 845–866.

Niinemets Ü., Kull O. & Tenhunen J.D. (1998) An analysis of light effects on foliar morphology, physiology, and light interception in temperate deciduous woody species of contrasting shade tolerance. *Tree Physiology* **18,** 681–696.

Nishio J.N., Sun J. & Vogelmann T.C. (1993) Carbon fixation gradients across spinach leaves do not follow internal light gradients. *Plant Cell* **5,** 953–961.

Oja V. & Laisk A. (2000) Oxygen yield from single turnover flashes in leaves: non-photochemical excitation quenching and the number of active PSII. *Biochimica et Biophysica Acta* **1460,** 291–301.

Oja V., Bichele I., Hüve K., Rasulov B. & Laisk A. (2004) Extinction coefficient of $P700^+$ at 810–950 nm in leaves. *Biochimica et Biophysica Acta* **1658,** 225–234.

Oja V., Eichelmann H., Peterson R.B., Rasulov B. & Laisk A. (2003) Decyphering the 820 nm signal: redox state of donor side and quantum yield of photosystem I in leaves. *Photosynthesis Research* **78,** 1–15.

Osmond C.B., Anderson J.M., Ball M.C. & Egerton J.J.G. (1999) Compromising efficiency: the molecular ecology of light-resource utilization in plants. In *Physiological Plant Ecology. The 39th Symposium of the British Ecological Society* (eds M.C. Press, J.D. Scholes & M.G. Barker) pp. 1–24. Blackwell Science Publishers, Oxford, UK.

Pearcy R.W. (1998) Acclimation to sun and shade. In *Photosynthesis: a Comprehensive Treatise* (ed. A.S. Raghavendra), pp. 250–263. Cambridge University Press, Cambridge, UK.

Peterson R., Oja V. & Laisk A. (2001) Chlorophyll fluorescence at 680 and 730 nm and its relationship to photosynthesis. *Photosynthesis Research* **70,** 185–196.

Reich P.B., Walters M.B. & Ellsworth D.S. (1997) From tropics to tundra: Global convergence in plant functioning. *Proceedings of the National Academy of Sciences of the USA* **94,** 13730–13734.

Terashima I. (1989) Productive structure of a leaf. In *Photosynthesis Proceedings of the C S. French Symposium on Photosynthesis held in Stanford, California, July 17–23, 1988* (ed. W.R. Briggs), pp. 207–226. Alan R. Liss, Inc., New York, USA.

Terashima I. & Evans J.R. (1988) Effects of light and nitrogen nutrition on the organization of the photosynthetic apparatus in spinach. *Plant and Cell Physiology* **29,** 143–155.

Terashima I. & Hikosaka K. (1995) Comparative ecophysiology of leaf and canopy photosynthesis. *Plant, Cell & Environmrnt* **18,** 1111–1128.

Theobald J.C., Mitchell R.A.C., Parry M.A.J. & Lawlor D.W. (1998) Estimating the excess investment in ribulose-1,5-bisphosphate carboxylase/ oxygenase in leaves of spring wheat grown under elevated CO_2. *Plant Physiology* **118,** 945–955.

Vernon L.P. (1960) Spectrophotometric determination of chlorophylls and pheophytins in plant extracts. *Analytical Chemistry* **32,** 188–194.

Walters R.G., Rogers J.J.M., Shephard F. & Horton P. (1999) Acclimation of *Arabidopsis thaliana* to the light environment: the role of photoreceptors. *Planta* **209,** 517–527.

Warren C.R., Adams M.A. & Chen Z. (2000) Is photosynthesis related to concentrations of nitrogen and Rubisco in leaves of Australian native plants? *Australian Journal of Plant Physiology* **27,** 407–416.

Woodward F.I., Smith T.M. & Emanuel W.R. (1995) A global land primary productivity and phytogeography model. *Global Biogeochemical Cycles* **9,** 471–490..

Received 1 April 2004; received in revised form 23 September 2004; accepted for publication 27 September 2004